Journal of Physics: Conference Series

PAPER • OPEN ACCESS

Design and Development of a Low-Cost Magnetic Induction Spectroscopy (MIS) Instrumentation

To cite this article: Tushar Kanti Bera and Toushik Maiti 2020 *J. Phys.: Conf. Ser.* **1495** 012003

Design and Development of a Low-Cost Magnetic Induction Spectroscopy (MIS) Instrumentation

Tushar Kanti Bera[1*], Toushik Maiti[1]

[1]National Institute of Technology Durgapur (NITDgp), Durgapur, WB 713209, India

E-mail: tkbera77@gmail.com

Abstract: Design and development procedure of a low-cost Magnetic Induction Spectroscopy (MIS) instrumentation has been presented. Along with the mathematical model of the electromagnetic system, MIS instrumentation is developed with two windings of suitable turns using enamelled copper wires of required cross-sectional area. The variable voltage multifrequency function generator developed to generate the magnetic field lines is used to excite the primary coil. The voltage developed at the secondary winding due to the Faraday's electromagnetic induction principle is acquired to sense the permeability of the different materials placed as the core of the electromagnetic interface. The SNR has been studied for different amounts of voltages and frequencies of the electrical excitation applied at primary winding. The advantages and limitations of the system have been described along with the future work and possible applications of the system.

Keywords: Magnetic Induction Spectroscopy (MIS), Non-destructive testing (NDT), MIS instrumentation, material characterization, signal to noise ratio (SNR).

1. Introduction

Non-Destructive Testing (NDT) [1-2] is a non-invasive technique for doing inspection, testing and evaluating the material properties without causing any harm to the materials. NDT can help us not only to inspect and control the manufacturing processes, but also provides the online and offline material characterization even in the wireless mode to test the material installed or working in remote area. Magnetic Induction Spectroscopy (MIS) [3-5] is a NDT technique that could be applied in different areas of engineering, technology, and other applied sciences. The MIS system consists of three main parts: electrical signal generation instrumentation (ESGI), electromagnetic interface (EMI) system and subject under test (SUT). The MIS technique is found promising for different fields of applications such as biomedical engineering [6-7], industrial engineering [8], defence and security [9] and so on, but the design of an ESGI needs to be studied in detail. As the MIS system is a non-contact material characterization system, the signal to noise ratio (SNR) of the system is found to be reduced for unwanted interference. Therefore, for an MIS system, the design of the ESGI is very crucial. The works presenting the detail design aspects of the ESGI of an MIS system are still required to be explored. This paper has presented the design, development, and testing of a low-cost MIS instrumentation and the frequency response of the secondary voltage for a coplanar coil assembly. MIS instrumentation is developed with two coplanar circular windings of suitable turns using enamelled copper wires of required cross-sectional area. The variable voltage multifrequency function generator developed to generate the magnetic field lines is used to excite the primary coil. The voltage developed at the secondary winding due to the Faraday's electromagnetic induction principle is acquired to sense the permeability of the different materials placed as the core of the electromagnetic interface. The SNR has been studied for different amounts of voltages and frequencies of the electrical excitation applied at primary winding. The advantages and limitations of the system have been described along with the future work and possible applications of the system.

2. Materials and Method

2.1 MIS as an NDT Technique

Depending on the signal used in NDT, it can be of several types such as electrical, magnetic, optical, acoustic, or else. In NDT, spectroscopic methods which apply a signal or energy to collect the system responses at a number frequency are found very promising as the frequency response of the system property (transfer function) is obtained as the signature of the material characteristics. A number of spectroscopic techniques have been proposed for material characterization such as Electrical Impedance Spectroscopy (EIS) [10-12], Magnetic Resonance Spectroscopy (MRS) [13-14]. Magnetic Induction Spectroscopy (MIS), one of the spectroscopic methods, uses electromagnetic induction principle to measure the passive electrical properties (PEP) such as electrical conductivity (σ), magnetic permeability (ϵ) and absolute permittivity (μ) of the sample at various operating frequencies. EIS, which is found as one of the very efficient spectroscopic techniques, has been used in various fields of applied science and engineering [15-18]. EIS injects constant amplitude alternating current signals to the sample under test and measures the electrical impedance of the SUT using two-electrode method [19] or four-electrode method [19]. The electrode-based bio-impedance techniques [19] such as EIS, electrical impedance tomography (EIT) [20-23], electrical impedance cardiography [24], electrical impedance plethysmography [25] all need surface electrodes to be properly fixed on the object boundary and hence suffer from contact impedance problems [19, 26]. Being an impedance measurement technique, the EIS also suffer from the limitations evoked from the electrode-subject interface and the contact impedance problem [19, 26]. On the contrary, MIS provides a fully non-contact non-invasive measurement thorough and electromagnetic coupling instead of galvanic coupling between sensors and samples. Moreover, as the magnetic field can penetrate many objects and all kind of tissues, MIS is particularly attractive for monitoring the brain properties to study the central nervous system. The MIS not only eliminates the problems produced by ill-defined electrode-skin interface, but also provides better patient safety due to the non-contact procedures.

2.2 MIS and Material Properties

In MIS, the electric energy is applied to a coil (called primary coil) and the potential developed in an another coil (called secondary coil) due to the electromagnetic induction is measured to calculate the σ, ϵ and μ (Fig. 1). Using magnetic induction based NDT techniques such MIS or magnetic induction tomography (MIT) [27] several properties of the material can be obtained such as magnetic permeability [27-29], electrical conductivity [27-28] and relative permittivity [27-28]. Using a magnetic core with primary and secondary coil (as shown in Fig. 1a), the magnetic permeality of the material (object under test) kept within the airgap can be assessed. If relative permeability of the core μ_{ic} is very large compared to that of the μ_{ag} and if the N_1, N_2, f and V_1 remain constant, (Fig. 1a), the permeability of the test object can be found in terms of the secondary voltage V_2 [30]:

$$|V_2| = k\frac{\mu_{ag}A_{ag}}{l_{ag}} \tag{1}$$

Using MIS technique, the electrical conductivity information of the material can also be obtained using a suitable MIS instrumentation as shown below [31]. Like other homogeneous, linear, isotropic and nonmagnetic material, the biological tissue can be characterized using MIS. The electrical conductivity of the biological tissues could also be measured using a basic MIS measurement system as shown in Fig. 1b. In this MIS system, the tissue sample kept between the primary coil and secondary coil which work as an excitation coil and detecting coil respectively. The signal detected by the secondary coil is contributed by two components [27]: first one is directly induced by the primary field (B) and the second one is the field developed by the eddy currents (ΔB) generated within the sample. If the skin depth of the electromagnetic field in the tissue is large compared to the thickness of the tissue sample, the ratio between B and ΔB is proportional to the conductivity of the sample and the frequency of the system [27, 30-31].

$$\frac{\Delta B}{B} \propto \omega\sigma \tag{2}$$

Therefore, the magnitude of the field ΔB is found normally proportional to the conductivity of the sample and the frequency of the system. In this paper, a basic MIS set up has been developed with a copper coil assembly connected with a sinusoidal signal source and a voltage measuring device. The effect of the frequency variation on the secondary coil voltage is studied for different coil diameter, different coil turns and different core materials. The following subsections will discuss in detail about the MIS instrumentation developed with a coplanar copper coil assembly.

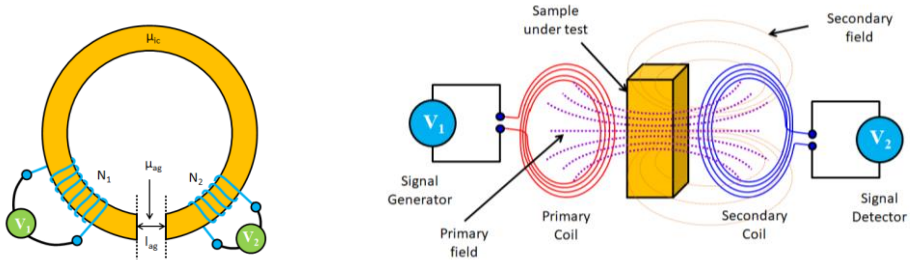

Fig. 1. (a) MIS systems for (a) permeability measurement [30], (b) conductivity measurement [31].

2.3. MIS Instrumentation:

The MIS system instrumentation has been developed using a magnetically coupled copper coil assembly, a voltage generation unit and a voltage measuring device. The air cored copper coil assembly is developed with two circular coils called a primary coil (Fig. 2a) and a secondary coil (Fig. 2b) which are kept in a concentric and coplanar geometry. Sinusoidal oscillator, developed with MAX038 function generator IC, is used to excite the primary coil and the secondary voltage signals are measured with a digital storage oscilloscope. The MIS coil assembly consists of two circular coils (Fig. 2): a primary coil (Fig. 2a) and a secondary coil (Fig. 2b), which are developed with 18 AWG enameled copper wire. Primary windings are developed with circular shaped copper wire with an outer and inner diameter of 108 mm and 94 mm respectively.

Fig. 2. MIS Copper coils (a) primary coils (D_{1i} = 94 mm), (b) secondary coils (D_{2i} = 54 mm).

The outer and inner diameters of the secondary windings are set as 65 mm and 54 mm respectively. Both the primary and secondary windings are developed with circular shaped coils with different primary turn numbers (T_1) and different secondary turn numbers (T_2). For the present study both the primary and secondary winding are made up with 5, 10 and 20 turns. Primary coils are developed with a fixed inner diameter (D_{1i}) of 94 mm and secondary coils are developed with a fixed inner diameter (D_{2i}) of 54 mm. Different concentric and coplanar coil assemblies are developed by varying the T_1 and T_2. The primary coil is fed by a voltage controlled oscillator (VCO) and the secondary coil is connected to a digital storage oscilloscope (TDS1001B, Dual Channel, 40 MHz, 500MS/s, Tektronix Inc., USA). The frequency response of the magnetic induction and secondary voltage variation is studied (Fig 3a) for different coil assembly, two different core materials (Fig.3b-3c) denoted by Object-1 and Object-2. Object-1 is a metal-plastic composite core material (USB based AC to DC Adapter as shown in Fig. 3b), whereas Object-2 is metal box with soldering paste as shown in Fig. 3c.

3. Results and Discussion

The secondary voltage is studied for 5, 10 and 20 turns with a primary coil developed with 20 turns and excited by a 1 V (RMS) sinusoidal signal for different frequencies. It is observed that the RMS values of the voltage V_2 becomes 46.7 mV, 99.1 mV and 205 mV for the number of turns 5, 10 and 20 respectively in secondary winding (Table 1). As shown in Table 2, At 100 kHz the voltage V_2 becomes 50.4 mV, 106 mV and 220 mV for the number of turns 5, 10 and 20 respectively. Table 3 represents the secondary voltage data collected at 500 kHz. It is observed the voltage V_2 becomes 51.3 mV, 109 mV and 229 mV respectively for the number of turns 5, 10 and 20. V_2 becomes 51.6 mV, 111 mV and 247 mV for the number of turns 5, 10 and 20 respectively at 1 MHz (Table 4).

Fig. 3: (a) MIS experimental set up with 20:20 coil assembly, (b) object 1, (c) object 2.

The frequency response of the secondary RMS voltage for different core material with a turn ratio of 20:20 is studied and it is observed that the secondary voltage not only vary with the frequency as shown in the previous tables but also the frequency response differs for different materials. It is observed that, for air core system, the secondary voltage increases from 205 mV to 247 mV for a frequency change from 25 kHz to 1 MHz (Fig. 4). For a metal-plastic composite core material (USB based AC to DC Adapter as shown in Fig. 3), increases from 208 mV to 243 mV for a frequency change from 25 kHz to 1 MHz. When a metal box with soldering paste is used as a core material and frequency has been increased from 25 kHz to 1 MHz, the secondary voltage increases from 227 mV to 239 mV. It is observed that the rate of change of the secondary voltage over frequencies increases with the number of turns (Fig. 4a). Results show that the rate of increase in secondary voltage is low for 5 turns and increases as the turn number is made high. As shown in the Table 1 to Table 4, for 5 turns in secondary, the secondary voltage is found 46.7 mV, 50.4 mV, 51.3 mV and 51.6 mV at 25 kHz mV, 100 kHz, 500 kHz and 1 MHz respectively (Fig. 4b). Thus, a saturation effect is observed at high frequency (over 500 kHz). The saturation effect over frequency decreases as the number of turns increases in the secondary coil. As shown in Fig. 4b, the saturation phenomena is found less for 10 turns in the secondary winding, because for 25 kHz mV, 100 kHz, 500 kHz and 1 MHz, the secondary voltages are noted as 99.1 mV, 106 mV, 109 mV and 111 mV respectively. Similarly, for the further increase in number of turns in the secondary, the rate of saturation decreases and the secondary voltage did not saturate till 1 MHz (Fig. 4b). It is noticed that, for 20 turns in the secondary coil, the secondary voltage is found 205 mV, 220 mV, 229 mV and 247 mV at 25 kHz, 100 kHz, 500 kHz and 1 MHz respectively. The SNR has been tested with the coil assembly with a turn's ratio of 20:20. The results demonstrate that SNR of the instrumentation system developed is found as 54.78 dB, 53.07 dB and 52.21 dB at 25 kHz, 50 kHz and 100 kHz respectively.

Table 1. Secondary RMS voltage for different number of turns in secondary coil at 25 kHz

Sl. No	Frequency (kHz)	Transformation Ratio	Secondary Voltages (mV)
1	25	20/05	46.7
2	25	20/10	99.1
3	25	20/20	205

Table 2. Secondary RMS voltage for different number of turns in secondary coil at 100 kHz

Sl. No	Frequency (kHz)	Transformation Ratio	Secondary Voltages (mV)
1	100	20/05	50.4
2	100	20/10	106
3	100	20/20	220

Table 3. Secondary RMS voltage for different number of turns in secondary coil at 500 kHz

Sl. No	Frequency (kHz)	Transformation Ratio	Secondary Voltages (mV)
1	500	20/05	51.3
2	500	20/10	109
3	500	20/20	229

Table 4. Secondary RMS voltage for different number of turns in secondary coil at 1000 kHz

Sl. No	Frequency (kHz)	Transformation Ratio	Secondary Voltages (mV)
1	1000	20/05	51.6
2	1000	20/10	111
3	1000	20/20	247

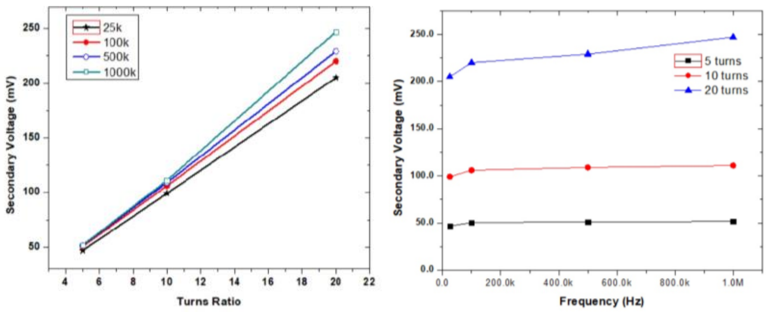

Fig. 4: (a) Secondary voltage for different turn ratios in the secondary with a primary coil with 20 turns, (b) Secondary voltage for different frequencies with a turn ratios of 5, 10 and 20.

4. Conclusions

A magnetic induction spectroscopy system instrumentation is developed and the frequency response of the magnetic induction and secondary voltage variation is studied for different coil assembly, different core materials. Results demonstrate that the MIS instrumentation is suitable to study the magnetic coupling and the voltage transfer between the coil and a future application for conductivity measurement. MIS studies conducted with different core materials showed that the secondary voltage response varies with different core materials. The voltage variation between air cored and the non-air cored geometries also differ with frequencies. It is observed that the rate of change of the secondary voltage over frequencies increases with the number of turns. Results show that the rate of increase in secondary voltage is low for 5 turns and increases as the secondary turn number is increased. A saturation effect is observed at high frequencies (over 500 kHz). Results show that, the value, at which the saturation effect occurs, increases as the number of turns increases in the secondary coil. It is observed that for 20:20 turn ratio, the saturation does not appear till 1 MHz. The MIS study conducted on a coplanar coil assembly show that the permeability variation is reflected within the secondary voltage which could be analysed further to extract the permeability information. Future study will report about the conductivity data extraction from the MIS data available at the secondary and will be utilized to characterize the biological materials.

5. References

[1] Cartz, Louis. Nondestructive testing. (1995).
[2] Raj *et al*. Practical non-destructive testing. Woodhead Pub., 2002.
[3] Barai *et al.* Magnetic induction spectroscopy: non-contact measurement of the electrical conductivity spectra of biological samples. Meas. Sc. and Technol. 23.8 (2012): 085501.
[4] O'Toole *et al.* Non-contact multi-frequency magnetic induction spectroscopy system for industrial-scale bio-impedance measurement. Meas. Sc. and Technol. 26.3 (2015): 035102.
[5] González *et al.* Over-hydration detection in brain by magnetic induction spectroscopy. Journal of Physics: Conference Series. Vol. 224. No. 1. IOP Publishing, 2010.
[6] Scharfetter *et al.* Biological tissue characterization by magnetic induction spectroscopy (MIS): requirements and limitations. IEEE Trans. Bio-Med Eng. 50.7 (2003): 870-880.
[7] Hevia-Montiel, N, and E Sanchez-Soto. Early Breast Cancer Detection by Magnetic Induction Spectroscopy. Trans. of Japanese Society for Med. and Biol. Engg. 51. Supp (2013): R-196.
[8] O'Toole, Michael D., N. Karimian, and A.J. Peyton. Classification of nonferrous metals using magnetic induction spectroscopy. IEEE Trans Ind Inform. 14.8 (2017): 3477-3485.
[9] Won, I. J., Dean A. Keiswetter, and Thomas H. Bell. Electromagnetic induction spectroscopy for clearing landmines. IEEE Trans Geosci Remote Sens 39.4 (2001): 703-709.
[10] Macdonald, J. Ross. Impedance spectroscopy. Vol. 41. New York etc: Wiley, 1987.
[11] Bera *et al.* Electrical impedance spectroscopy (EIS)-based evaluation of biological tissue phantoms to study multifrequency electrical impedance tomography (Mf-EIT) systems. J. of Visualization 19.4 (2016): 691-713.
[12] Bera *et al.* Electrical impedance spectroscopy for electro-mechanical characterization of conductive fabrics. Sensors 14.6 (2014): 9738-9754.
[13] Jagannathan, *et al.* Brain metabolite changes in alcoholism: an in vivo proton magnetic resonance spectroscopy (MRS) study. Mag. Reso. Imaging 14.5 (1996): 553-557.
[14] Dager *et al.* Research applications of magnetic resonance spectroscopy (MRS) to investigate psychiatric disorders. Topics in Mag. Reso. Imaging: TMRI 19.2 (2008): 81.
[15] Dean *et al.* Electrical impedance spectroscopy study of biological tissues. Journal of electrostatics 66.3-4 (2008): 165-177.
[16] Bera, TK, and J. Nagaraju. Studying the resistivity imaging of chicken tissue phantoms with different current patterns in Electrical Impedance Tomography (EIT). Measurement 45.4 (2012): 663-682.
[17] Jüttner, K. Electrochemical impedance spectroscopy (EIS) of corrosion processes on inhomogeneous surfaces. Electrochimica Acta 35.10 (1990): 1501-1508.
[18] Almuhammadi *et al.* Electrical impedance spectroscopy for measuring the impedance response of carbon-fiber-reinforced polymer composite laminates. Composite Structures 168 (2017): 510-521.
[19] Bera, Tushar Kanti. Bioelectrical impedance methods for noninvasive health monitoring: a review. Journal of medical engineering 2014 (2014).
[20] Cherepenin *et al.* A 3D electrical impedance tomography (EIT) system for breast cancer detection. Physiological measurement 22.1 (2001): 9.
[21] Cao *et al.* A novel time-difference electrical impedance tomography algorithm using multi-frequency information. Biomedical engineering online 18.1 (2019): 84.
[22] Tommaso *et al.* Noninvasive assessment of airflows by electrical impedance tomography in intubated hypoxemic patients: an exploratory study. Ann. Intensive Care 9.1 (2019): 83.
[23] Bera, TK, and J. Nagaraju. A MATLAB-based boundary data simulator for studying the resistivity reconstruction using neighbouring current pattern. J. of Med. Engg. 2013 (2013).
[24] Patterson, Robert P. Fundamentals of impedance cardiography. IEEE Engineering in Medicine and Biology magazine 8.1 (1989): 35-38.
[25] Nyboer *et al.* Electrical impedance plethysmography: A physical and physiologic approach to peripheral vascular study. Circulation 2.6 (1950): 811-821.

[26] Roberto *et al.* Electrode contact impedance sensitivity to variations in geometry. Physiol. Meas. 33.5 (2012): 817.
[27] Griffiths, H. Magnetic induction tomography. Meas. Sci. Technol 12.8 (2001): 1126.
[28] Soleimani, Manuchehr. Simultaneous reconstruction of permeability and conductivity in magnetic induction tomography. J Electromagnet Wave. 23.5-6 (2009): 785-798.
[29] Baumangrep, John H., and Richard W. Hoffman. Magnetic susceptibility meter for in vivo estimation of hepatic iron stores. IEEE Trans. Bio-Med Eng. 4 (1967): 239-243.
[30] Zhang, Ziyi, Mohammed Ali Roula, and Richard Dinsdale. Magnetic Induction Spectroscopy for Biomass Measurement: A Feasibility Study. Sensors 19.12 (2019): 2765.
[31] Baumangrep, John H., and Richard W. Hoffman. Magnetic susceptibility meter for in vivo estimation of hepatic iron stores. IEEE Trans. on Biomed. Engg. 4 (1967): 239-243.